Modeling and Model Verification of an Intelligent Self-Balancing Two-Wheeled Vehicle for an Autonomous Urban Transportation System

Michael Baloh and Michael Parent
INRIA/IMARA Domaine de Voluceau, B.P. 105
78153 Le Chesnay Cedex, France
{michael.baloh,michel.parent}@inria.fr

Abstract

This paper presents a brief summary of the first stage of control work for an intelligent two wheeled road vehicle called the B2. Originally conceived within the CyberCars Project, the intended goal of the B2 is to provide an on-demand, fully automatic taxi service in an urban environment. The B2, like the Segway, is principally a self balancing machine whose wheels share a common axis. However, the control objective are different since the intended use of the two vehicles are unalike; The Segway longitudinal acceleration and thus velocity are controlled by the torque disturbance of the driver. Thus, when a driver leans forward, the Segway accelerates forward to prevent the passenger from falling. This is the typical response of an inverted pendulum. In contrast, the B2 trajectory must be entirely controlled by the steering computer. Thus, the passenger motion is a disturbance to be rejected. Furthermore, the B2 is meant as an alternative road vehicle, not intended for the sidewalk. This article outlines the work to understand the fundamental problems of engineering the B2. In particular, we create a mathematical model of the vehicle dynamics and use open loop and closed loop experiments for verification purposes.

1 Introduction

In this paper, we study a very fundamental question about vehicle technology. Specifically, are there alternative approached to the basic automobile platform? Consider that with almost no exception, all modern vehicles are four wheeled boxes. Perhaps this was the only practical geometry until recently, however, with recent advances in control theory and electronics, it has become possible to consider radical alternatives. For instance a two wheeled self-balancing vehicle. Although radical, this idea is not entirely new. As early as 1912, balancing passenger vehicles where in existence [13] which were made stable by massive gyroscopes. More recently, Yuta [9, 12] has devoted much work to the problem of two wheeled robots to improve maneuverability and reduce size. Our own motivation for developing a two wheeled vehicle is an outgrowth of the European project called CyberCars [15, 18]. The goal of this project is to improve urban living by reducing pollution and congestion associated with the transportation needs of a modern society. Recent studies of shown that the automobile can extremely competitive with all other form

Figure 1: The B2 as envisioned for public service. The vehicle is equipped with two seats and a computer. The screen allows the user to easily and in an interactive way, enter desired destination and monitor transit status.

of public transportation for energy efficiency [4]. To take advantage of this observation while reducing the pollution and congestion associated with automobiles is the principle target of our work. The majority of our vehicles for the pilot program [16] are of the conventional type. However, the initial cost, size, and maintenance problems are problematic. The impetuous to design a two wheeled road vehicle follows from this experience. The sum of the opposing wheel speed dictates longitudinal speed while differential wheel speed gives direction. Thus, the weight, complexity, and cost of steering mechanisms disappear. In addition, the B2 can rotate on itself, thus making it highly maneuverable in European city centers (of which several are limiting or entirely restricting access to cars). Finally, the total size of the B2 is such that 10 can fit into the space of one ordinary car. Thus, the two wheeled vehicle concept is highly compatible with our main intentions. Figure (1) shows an image of our concept of a two wheeled road vehicle.

The nature of this two wheeled vehicle poses several interesting controls questions. For instance, while a person occupies the vehicle, their movements change the vehicle center-of-gravity. Consequently, if the standard inverted pendulum control were to be applied the control algorithm would be obliged to maintain a steady acceleration to achieve the control objective [14, 2, 3] This appears to be the principle means of controlling the Segway. However, as already stated, this is not compatible with our final objectives. As such, a control algorithm must be found which seeks the natural equilibrium point of the system, thus rejecting passenger motion so that speed can be automated.

Judging by the model, the balance problem of the B2 appears to be a linear one since the pitch of the vehicle is restricted to be $\leq 15^o$ and inertial damping limits the pendulum body (up to $12kg - m^2$) rotations. Both facts which mitigate nonlinearities common to inverted pendulums [17, 8]. However, the mass and placement of the occupants will normally be unknown so any control applied should address uncertainty explicitly.

On the other hand, the occupants aren't simply parametric uncertainty, instead they represent both unmodeled dynamics and disturbance. In part they react to the behavior of B2; when it stops suddenly they move forward. Simultaneously, they are true disturbance which may at any time perform an action which impacts B2 dynamics. Consequently, it will be seen that the balance command of the B2 falls into the category of robust linear controls such as μ-synthesis [6, 19]. Ironically, to make good use of robust control and achieve good results, one is obliged to characterize the uncertainty of the plant. Often this requires a detailed experimental study to identify the plant.

Hence, this article deals with modeling and identification of the vehicle. First, we briefly outline a 3D mathematical model of the B2 which was developed. Second, we conduct an open-loop experiments of the stable unloaded vehicle whose center-of-mass below the wheel axle. This has the advantage of giving us detailed model information before introducing unknown moments due to passengers. Later works will build on these results by implementing a preliminary LQR and conducting closed-loop experiments to accurately characterize machine dynamics.

2 Dynamic Model of the B2

The dynamic model of the B2 is now presented. The basis of the model is a 3D vehicle carrying a rigid mass load as illustrated in Figure (2). Several simplifying assumption are made which are important. First, a no-slip condition is placed on the wheels (A1). Second, the vehicle body composed of chassis and persons are assumed to be a single rigid body (A2). Third, the vehicle is assumed to operate on a relatively flat surface so that rolling motion is not possible (A3). The first assumption provides the necessary conditions for a kinematic model which connects wheel motion to inertial forces which act on the inverted body (the principle mechanism of pendulum stabilization). The second assumption will be justified or modified based on observations. The third assumption is justified restricting the vehicle to 20% grades (about 11^o). Still, it may be worth further consideration in the future since turning the vehicle on an incline causes the pendulum to experience a rolling motion.

2.1 Lagrangian Equations and nonlinear model

Model development is straightforward and calculated by the Lagrangian Method [5]. Working from left diagram of Figure (2) we write the coordinates for the point intermediary between the two wheels of B2

$$\begin{aligned} \dot{x} &= \frac{R}{2}(\dot{\theta}_{lw} + \dot{\theta}_{rw})sin(\phi) \\ \dot{y} &= -\frac{R}{2}(\dot{\theta}_{lw} + \dot{\theta}_{rw})cos(\phi) \\ \dot{\phi} &= \frac{R}{W}(\dot{\theta}_{lw} - \dot{\theta}_{rw}) \end{aligned}$$

Where the subscript notation is described in Figure (2). Note that if we define $\phi(t = 0) = 0$ then we have as a direct constraint on rotation $\phi = (R/W)(\theta_{lw} - \theta_{rw})$. Given the center position of the vehicle in the xy-plane the wheels positions are given as

$$\begin{aligned} x_{lw} &= x - \frac{W}{2}cos(\phi) \qquad x_{rw} = x + \frac{W}{2}cos(\phi) \\ y_{lw} &= y - \frac{W}{2}sin(\phi) \qquad y_{rw} = y + \frac{W}{2}sin(\phi) \end{aligned}$$

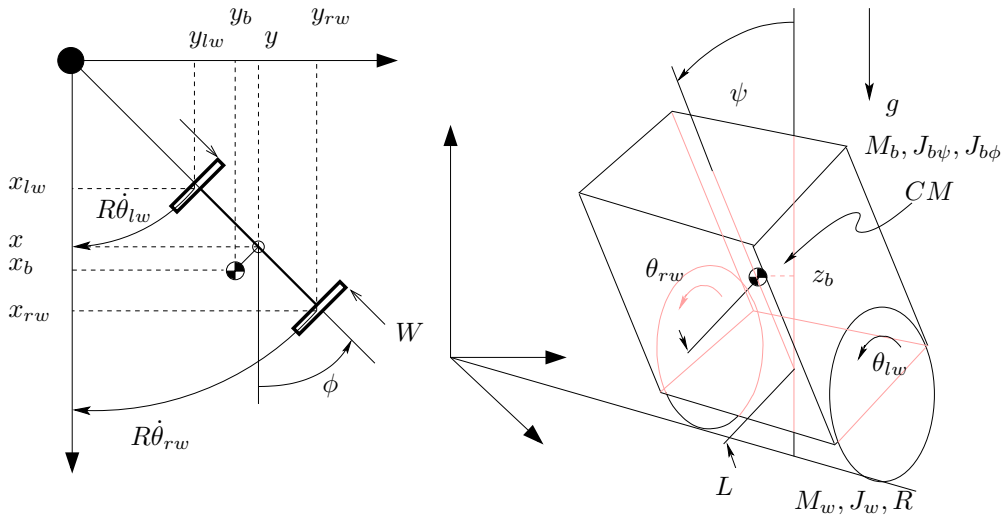

Figure 2: Illustrations of the kinematic (left) and dynamic (right) models for the B2 operating on a plane with a effective pendulum height of z_b. The pendulum body swings about the ψ-axis and the entire vehicle can rotate in xy-plane about the ϕ-axis. There are three dimensions of significance: L, R, and W which are the effective the pendulum length, wheel radius, and wheel base. Masses are designated by M and moments as J. Subscripts are $b\psi$, $b\phi$, correspond to body moment about ψ and ϕ axes. Subscripts lw and rw indicate either left or right wheel moment or masses. Several assumptions have been made. First, that the vehicle operates only on a flat surface. Second, that the rotation of the wheels is proportional to longitudinal speed (no-slip). Third, that the passengers and body of the vehicle behave as a rigid body with center-of-mass (CM). Occupant movement can be modeled as a torque disturbance along the ψ axis.

and the body position (CM)

$$\begin{aligned} x_b &= x + Lsin(\phi)sin(\psi) \\ y_b &= y - Lcos(\phi)sin(\psi) \\ z_b &= R + Lcos(\psi) \end{aligned}$$

Where L is the distance of the center-of-mass from the wheel axle as illustrated in Figure (2). Given the kinematics of the vehicle components, it is is a straightforward process to write the energy expression for the complete plant

$$\mathcal{L} = T^* - V = \frac{1}{2}(\dot{\Psi}^T \mathbf{J} \dot{\Psi} + \dot{X}^T \mathbf{M} \dot{X}) - \mathbf{M}\,(g \cdot X)$$

Where Ψ and X are translational and rotational coordinates defined as

$$\Psi = (\psi, \phi, \theta_{lw}, \theta_{rw}, \eta(\theta_{lw} - \psi), \eta(\theta_{rw} - \psi)^T$$

and

$$X = (x_{lw}, y_{lw}, x_{rw}, y_{rw}, x_b, y_b, z_b)^T$$

The matrices $\mathbf{J}$ and $\mathbf{M}$ are the moments and masses of the vehicle. In our case, they are simply diagonal matrices given as

$$\mathbf{J} = \text{diag}(J_{b\psi}, J_{b\phi}, J_w, J_w, J_m, J_m)$$

and

$$\mathbf{M} = \text{diag}(M_w, M_w, M_w, M_w, M_b, M_b, M_b)$$

Examination of the variable $\mathcal{L}$ shows that there are three independent variables, which we use to define the generalized coordinate vector $q = (\theta_{lw}, \theta_{rw}, \psi)$. The equations of motion can then be derived from the Lagrangian equations

$$\frac{d}{dt}\left(\frac{\partial \mathcal{L}}{\partial \dot{q}_i}\right) - \frac{\partial \mathcal{L}}{\partial q_i} = \Xi_i \quad \text{i=1,2,3} \tag{1}$$

Here Ξ_i are generalized forces acting parallel to each independent coordinate. These are used to describe external or internal, conservative or nonconservative forces necessary to express the model [5]. Since the variations δq_i are independent, the generalized forces f_i can be calculated from the equations

$$\Xi_i = \sum_{j=1}^{N} f_j \cdot \frac{\partial R_j}{\partial q_i} \quad \text{i=1,2,3}$$

This calculation is necessary to generate correct forcing functions for the motor torque as well as damping matrices due to gearbox and tire friction. Evaluating Eqs. (1) we derive the following dynamic equations which we place in the form

$$\mathbf{H}(q)\ddot{q} + \mathbf{C}(q, \dot{q})\dot{q} + \mathbf{G}(q) = \mathbf{Q}u \tag{2}$$

The mass matrix is found to be

$$\mathbf{H}(q) = h_a \begin{bmatrix} h_0 & h_1 & h_2 \\ h_1 & h_0 & h_2 \\ h_2 & h_2 & h_3 \end{bmatrix} + \begin{bmatrix} -h_c & h_c & h_b \\ h_c & -h_c & h_b \\ h_b & h_b & 0 \end{bmatrix}$$

with coefficients $h_a = 1/(4W^2)$, $h_b = LRM_b cos(\psi)/2$, and $h_c = L^2R^2M_b cos(2\psi)/(2W^2)$ and elements defined as

$$\begin{aligned} h_0 &= (4M_wW^2 + 4J_{b\phi} + (2L^2 + W^2)M_b)R^2 + \\ &\quad 4W^2(J_m\eta^2 + J_w) \\ h_2 &= -4W^2\eta^2 J_m \\ h_1 &= (M_b(W^2 - 2L^2) - 4J_{b\phi})R^2 \\ h_3 &= 4W^2(M_bL^2 + J_{b\psi} + 2\eta^2 J_m) \end{aligned}$$

The nonlinear damping matrix is a comprised of gyroscopic and damping

$$\mathbf{C}(q,\dot{q}) = c_a \begin{bmatrix} 1 & -1 & -\frac{W^2 sec(\psi)}{4LR} \\ -1 & 1 & -\frac{W^2 sec(\psi)}{4LR} \\ \frac{(\dot{\theta}_{rw} - \dot{\theta}_{lw})}{2\dot{\psi}} & \frac{(\dot{\theta}_{lw} - \dot{\theta}_{rw})}{2\dot{\psi}} & 0 \end{bmatrix} + \begin{bmatrix} \beta_{gb,lw} + \beta_t & 0 & -\beta_{gb,lw} \\ 0 & \beta_{gb,rw} + \beta_t & -\beta_{gb,rw} \\ -\beta_{gb,lw} & -\beta_{gb,rw} & \beta_{gb,lw} + \beta_{gb,rw} \end{bmatrix}$$

where $c_a = \frac{L^2R^2M_b sin(2\psi)\dot{\psi}}{W^2}$. The terms labeled β represent plant friction. Due significant causes are the gearboxes and tires which are indicated by subscripts gb and t. The principle cause of instability of the pendulum is because of the negative nonlinear stiffness nonlinear stiffness due to gravity

$$\mathbf{G}(q) = (0, 0, -gLM_b sin(\psi))^T$$

Finally, motors at each wheel can apply torque which provides a means of controlling vehicle speed and pendulum attitude

$$\mathbf{Q}u = \eta K_{mot} K_{da} \begin{bmatrix} K_{amp,lw} & 0 \\ 0 & K_{amp,rw} \\ -K_{amp,lw} & -K_{amp,rl} \end{bmatrix} \begin{Bmatrix} u_{lw} \\ u_{rw} \end{Bmatrix}$$

Here K_{amp} represents the amplifier which is modeled as a simple gain because they have bandwidth greater then 1kHz. While K_{mot} and K_{ad} are the motor torque constant and AD converter gain respectively.

The crucial state for this control problem is CM attitude ψ. This is the angle subtended by the gravity vector and the vector connecting the wheel axis and CM. There is no simple way to measure it directly. For example, measuring the distance from the ground to the bottom of the body would not be useful since this value is independent of the CM. (the terrain may not be flat). Another alternative would be to use an accelerometer as a tilt sensor. However the measurement is a complicated function of the body tilt, vehicle motion, and sensor position. Instead the B2 uses a gyroscope with gain K_{gyro} to measure the tilting rate of the CM $\dot{\psi}$. As a measurement sensor, gyroscope are largely independent of vehicle accelerations and entirely independent of sensor position. On the other hand, A notable disadvantage of the sensor is susceptibility to very low frequency noise in the form of temperature drift. Even so, the frequency range of the drift is on the order of minutes, whereas the response of the body dynamics in the range of fractions of seconds. Therefore, an effective technique is to apply a very low frequency high pass filter to the gyroscope output.

Vehicle speed is estimated by encoders K_{enc} attached to each motor rotor (thus further amplified by the gearbox ratio η) and anchored to the vehicle body. Since both the stator and rotor of the encoder are subject to rotation, the encoder registers the value $\theta - \psi$ and not simply the wheel speed.

Rotation about the ϕ can be accessed by measuring the difference of the wheel encoders (valid by the no-slip assumption A1). However, this would be inherently noisy. In addition, although great precision is not needed for control of the vehicle, it is desirable to have good odemetric estimates. This goal can be achieved by use of gyroscopes in conjunction with encoders as described by Borenstein [11, 10]. Consequently, a second gyroscope is mounted along the ϕ-axis. So that the measurement is consistent with the model, it is written as $K_{gyro}\frac{R}{W}(\theta_{lw} - \theta_{rw})$.

Thus, the B2 has the following partial state measurement capabilities

$$y = (\eta K_{enc}(\dot{\theta}_{lw} - \dot{\psi}), \eta K_{enc}(\dot{\theta}_{rw} - \dot{\psi}), K_{gyro}\dot{\psi}, K_{gyro}\frac{R}{W}(\theta_{lw} - \theta_{rw}))^T$$

Finally, some elaboration in the definitions of M_b, L, $J_{b\psi}$, and J_{b_ϕ} is necessary. Each of these values depends on the number of passengers N_p and their mass M_p. For our work, we compute the mass and pendulum length parameters by the formula

$$M_b = M_{b0} + N_pM_p \quad \text{and} \quad L = \frac{N_pM_pL_p + M_{b0}L_{b0}}{N_pM_p + M_{b0}}$$

Here L_p and L_{b0} are the distances from the passenger and unloaded vehicle center-of-masses to the wheel axle. The unloaded mass of the vehicle is assigned the constant M_{b0}. The moments $J_{b\psi}$ and $J_{b\phi}$ also depend on the passengers

$$J_{b\psi} = J_{b0\psi} + J_p \quad \text{and} \quad J_{b\phi} = J_{b0\phi} + J_p$$

where are passenger moments are found by standard approximations of rigid bodies [5]

$$J_{p\psi} \approx \frac{N_p M_p}{12} H_p^2 + N_p M_p L_p^2 \quad \text{and} \quad J_{p\phi} \approx \frac{N_p M_p}{12} W_p^2$$

where H_p and W_p are seated height and width of passengers. Although not addressed in this paper, it should be evident that from these equations that closed-loop performance is dependent on how well these uncertainties can be accounted for in the control design.

3 Open-Loop Model Identification and validation

As commented in the introduction, we wish to apply robust control techniques to the control of the B2. A necessary step in this process is to be able to characterize the plant model. In this paper we only consider identification where $N_p = 0$ and open-loop is stable (M_{b0} rests below the wheel axle). To this end, the following plan was executed

i. Characterize sensor and actuator gains.

ii. Identify wheels and drive train parameter with body off the ground.

iii. Measure I/O open-loop transfer function of entire unloaded and passive stable vehicle on special test bed.

iv. Validate complete open-loop system model.

During the first validation iteration, it became evident that the friction characteristics of the gearboxes played a significant role in the dynamic behavior of the vehicle. Consequently, it was necessary to make a nonlinear identification of the gear friction by the formula

$$\beta(\theta) = \tau + J\ddot{\theta}$$

The experiment was carried out by using a PID to regulate the speed of the wheel for constant speeds. Although a constant open-loop torque might have been applied, it was found that friction limited the ability to make very small rotational speed measurements because of "stick-slip" action. The basic experimental procedure for estimating the friction *at speed* was taken from [7]. To identify the stiction, or break-away torque, a method proposed by Armstrong [1] was used. Figure (3) shows friction speed curves calculated from the described method. Repeatability of the experiments was tested by remeasuring on different days and temperatures and found to be withing 2.5% for the left gearbox, and 5.3% for the right gearbox. With the exception of the gearbox friction, plant identification step $i - iii$

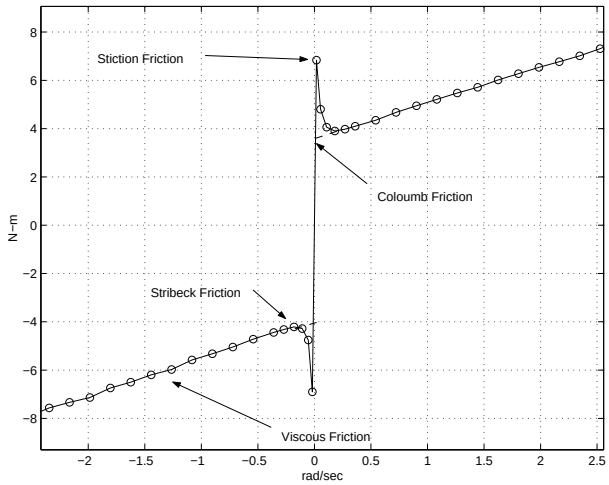

Figure 3: Measured friction model for the B2 Left motor (similar to right motor). As can be seen, the stiction friction is approximately $7N - m$, the Coulomb friction is about $4N - m$, and the viscous friction is about $1.4N - m/rad/sec$.

were completed and used to identify the model parameters of Eq. (2). As a validation of the model, two tests were conducted. The results of these experiments are shown in Figures (4) and (5). In the Figure (4) an equal step input torque is applied to both wheels which excites planar motion in the plane of pendulum. In Figure (5) an *equal and opposite* torque is applied to each wheel resulting in a twisting motion.

We first consider the results of the planar validation. Examining the simulation and experimental trajectories, we see there are both strengths and weaknesses in the identification. A particular strength of the model is its ability to replicate the sudden arrest of the wheel encoder signals. This occurs when the speed of the low inertia wheel decreases sufficiently for stiction friction to freeze the gearbox. Once the gearbox locks $\dot{\theta} = \dot{\psi}$ and the encoder output is zero. However, as seen in the gyroscope signal, the body continues to oscillate. At this instant, the body-wheel system is rocking back and forth on the wheel bottom where the predominate form of damping being caused by wheel rolling resistance β_t. Another strength of the model is its ability to render a good approximation to the state $\dot{\phi}$ which is perpendicular to the excitation. The biggest weaknesses of the model are attributable to a poor understanding of gearbox and tire friction. In particular, gearbox friction during high rate transients which manifests in the encoder response being about as much as 15% actual values. While, tire damping is responsible for the under damped characteristic of the body-wheel system from 8 seconds on wards.

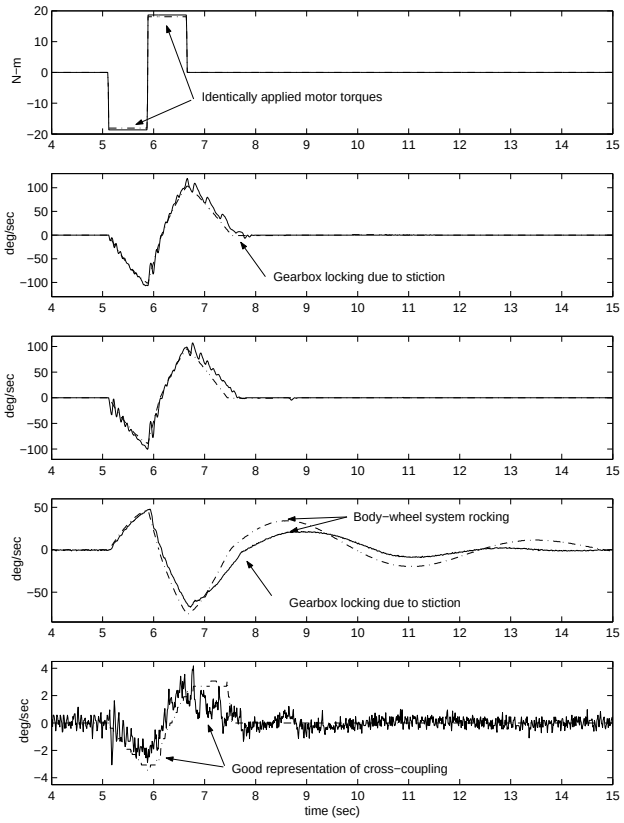

Figure 4: Validation experiment planar of dynamics. From top to bottom: Applied torque at each wheel $\eta\tau_{lw}$ (-) and $\eta\tau_{rw})$ (-.), left wheel encoder $\dot{\theta}_{lw}$, right wheel encoder $\dot{\theta}_{rw}$, $\dot{\psi}$ gyroscope output, and $\dot{\phi}$ gyroscope output . Experimental values are shows as a solid line and simulation as dashed (-.)

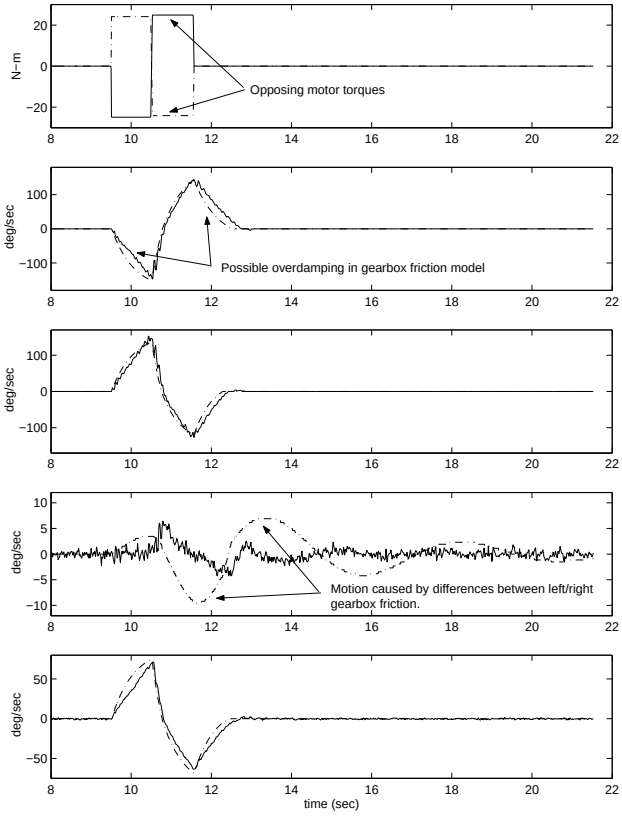

Figure 5: Validation experiment of twist (right) dynamics. From top to bottom: Applied torque at each wheel $\eta\tau_{lw}$ (-) and $\eta\tau_{rw})$ (-.), left wheel encoder $\dot{\theta}_{lw}$, right wheel encoder $\dot{\theta}_{rw}$, $\dot{\psi}$ gyroscope output, and $\dot{\phi}$ gyroscope output . Experimental values are shows as a solid line and simulation as dashed (-.)

Examining the twist validation experiment shown in Figure (5) yields additional insights into the model quality. Comparing the left and right encoders, we see that the left encoder shows an error of about 10% during transients although overall magnitude and phase appear good, while the right wheel is quite accurate for the entire period of the experiment. Consequently, the predicted behavior along $\dot{\phi}$ shows errors (recall that we have assumed $\dot{\phi}(\dot{\theta}_{lw}, \dot{\theta}_{rw})$) corresponding to weaknesses in the left wheel model. The most likely culprit is the gearbox friction which is difficult to estimate and model accurately during transients. This is further emphasized by the discrepancies between the simulation and experiment along ψ. During a twisting motion, besides inertial coupling, the body experiences a rotation about ψ dependent on the instantaneous differences in the left and right gearbox frictions. As can be seen, the model and simulation have little correlation.

In the end, the two weakness in the model prediction are due to tire damping and small differences in gearbox friction. However, it is unlikely that these might ever be modeled accurately. Furthermore, these errors represent mismodeling of weak off-diagonal terms and are dwarfed by the plant strong response of the diagonal terms. Thus, overall the quality of the fit can be made argued to be good since Figures (4) and (5) show strong agreement between plant simulation and experimental system.

4 Conclusions

In summary, we have developed a sixth order dynamic model of the B2 and dynamic and identified it experimentally. As a result we now have a simulation which accurately predicts the plant output trajectories and will allow us to make quick progress in control synthesis. In the next

phase of the project, we implement a simple LQR control. Although not ideal, this implementation allows us to quickly access the closed loop performance of the system. In particular, we are able to experiment with people mounted on the vehicle. Thus, we can learn how significant human mechanical properties (flexible modes) are to the control problem. Furthermore, we are able to repeat these experiments numerous times under different loads and conditions providing a tool for building an uncertainty model of the loaded B2. Therefore, from usage experience of the LQR command, control design specifications are revised to improve human-machine interaction.

References

[1] B. Armstrong. Friction: Experimental determination, modeling, and compensation. *Proceedings of IEEE International Conference on Robotics and Automation*, 3:1422–1427, 1988.

[2] K. Astrom and K. Furuta. Swinging up a pendulum by energy control. *IFAC 13th World Congress, San Francisco, California*, 1996.

[3] W. L. Brogan. *Modern Control Theory*. Prentice Hall, Englewood Cliffs, New Jersey 07632, 1991.

[4] R. Coffey and Lowson M.V. A comparative analysis of energy consumption and emission of urban transport systems. In Recio Eds. Baldasano and Sucharov, editors, *Urban Transport and the Environment II*. Computational Mechanics Publications, 1997.

[5] S. Crandall, D. Karnopp, E. Kurtz, and D. Pridmore-Brown. *Dynamics of Mechanical and Electromechanical Systems*. Krieger Publishing Company, Malabar, Florida, 1968.

[6] J. Doyle, B. Francis, and A. Tannenbaum. *Feedback Control Theory*. Macmillan Publishing Company, New York, 1992.

[7] E. Garcia, P. Gonzalez, and C Canudas de Wit. Velocity dependence in the cyclic friction arising with gears. *International Journal of Robotics Research*, 21(9):761–771, 2002.

[8] Kajiwara H., Apkarian P., and Gahinet P. lpv techniques for control of an inverted pendulum. *IEEE Control Systems*, 19(1):44–54, 1999.

[9] Yun-Su Ha and Shin'ichi Yuta. Trajectory tracking control for navigation of the inverse pendulum type self contained mobile robot. *Robotics and Autonomous Systems*, 17:65–80, 1996.

[10] Borenstein J. and Feng L. Gyrodometry: A new method for combining data from gyros and odometry in mobile robots. *Proceedings of the 1996 IEEE International Conference on Robotics and Automation*, pages 423–428, 1996.

[11] Borenstein J. and Feng L. Measurement and correction of systematic odometry errors in mobile robots. *IEEE Transactions on Robotics and Automation*, 12(6):869–880, 1996.

[12] E. Koyonagi, S. Iida, K. Kimoto, and S. Yuta. A wheeled inverse pendulum type self-contained mobile robot and its two-dimensional trajectory control. *Proc. of ISMCR'92*, pages 891–898, 1992.

[13] Baldwin N. *The Wolseley, ISBN 0747802971*. Shire Publications Ltd, Buckinghamshire, UK, 1995.

[14] Control of convey-crane based on passivity. J. collado and r. lozano and i. fontoni. *Prec. of the ACC, Chicago, Ill. June*, 2000.

[15] M. Parent. The cybercars. *ITS World Congress Chicago Oct 2002*, 2002.

[16] B. Saugy, K. Malone, and J.W. van der Wiel. Cybernetic transport systems: Lessons to be learned from user needs analysis and field experience. *IEEE Intelligent Vehicles Symposium*, 2002.

[17] M. Spong. The swing up control problem for the acrobot. *IEEE Control Systems*, February 1995.

[18] J. Uwland and M. Janse. Cybercars on the move. *Transport Matters, TNO Traffic and Transport Journal*, 2002.

[19] K. Zhou and J. Doyle. *Essentials of Robust Control*. Prentice Hall, Englewood Cliffs, New Jersey 07632, 1997.